Cell Reports
Resource

Morphological and Molecular Characterization of Adult Midgut Compartmentalization in *Drosophila*

Nicolas Buchon,[1,5,6,*] Dani Osman,[1,5,*] Fabrice P.A. David,[2] Hsiao Yu Fang,[4] Jean-Philippe Boquete,[1] Bart Deplancke,[3] and Bruno Lemaitre[1,*]
[1]Global Health Institute
[2]Bioinformatics and Statistics Core Facility
[3]Institute of Bioengineering
School of Life Sciences, Station 19, EPFL, 1015 Lausanne, Switzerland
[4]Department of Genetics, University of Cambridge, Cambridge CB2 3EH, UK
[5]These authors contributed equally to this work
[6]Present address: Department of entomology, Cornell University, Ithaca, NY 14850, USA
*Correspondence: nicolas.buchon@cornell.edu (N.B.), dani.osman@epfl.ch (D.O.), bruno.lemaitre@epfl.ch (B.L.)
http://dx.doi.org/10.1016/j.celrep.2013.04.001

SUMMARY

Although the gut is a central organ of Eumetazoans and is essential for organismal health, our understanding of its morphological and molecular determinants remains rudimentary. Here, we provide a comprehensive atlas of *Drosophila* adult midgut. Specifically, we uncover a fine-grained regional organization consisting of 14 subregions with distinct morphological, histological, and genetic properties. We also show that *Drosophila* intestinal regionalization is defined after adult emergence, remains stable throughout life, and reestablishes following acute tissue damage. Additionally, we show that this midgut compartmentalization is achieved through the interplay between pan-midgut and regionalized transcription factors, in concert with spatial activities of morphogens. Interestingly, disruption of the midgut compartmentalization leads to a loss of intestinal homeostasis characterized by an increase in stem cell proliferation and aberrant immune responses. Our integrative analysis of *Drosophila* midgut compartmentalization provides insights into the conserved mechanisms underlying intestinal regionalization in metazoans.

INTRODUCTION

The emergence of the gastrointestinal tract within the body cavity is one of the major innovations in animal evolution allowing the transition from an intracellular to an extracellular mode of digestion (Yonge, 1937; Terra, 1990; Stainier, 2005). In higher metazoans, the digestive tract further evolved into complex structures composed of successive and histologically distinct regions. Compartmentalization is an important feature of the digestive tract because it optimizes digestion by enabling sequential functions ranging from the uptake and processing of food, to nutrient absorption and elimination of solid waste (Karasov et al., 2011). Hence, understanding intestinal function requires an integrative analysis of the sequential organization of the gut.

To date, most studies on the gut have been devoted to understanding the genetic and cellular events required to specify and differentiate the embryonic gut primordium or to elucidate specific facets of adult gut physiology, such as the role of intestinal stem cells (ISCs) in epithelial renewal, the interaction between the mucosal immune system and microbiota, or the characterization of the brain-gut axis (Radtke and Clevers, 2005; Stainier, 2005; Pédron and Sansonetti, 2008). Although these studies have expanded our knowledge of the gut, a comprehensive, multiscale analysis describing and integrating the relationship between the structure and function of different gut regions is still lacking. Such a view is essential given that gut homeostasis is central to organismal health and that its disruption is associated with a broad range of pathologies ranging from inflammatory bowel disorders to intestinal cancers (Radtke and Clevers, 2005). Remarkably, most of these pathologies tend to be region specific, strongly suggesting that fine-grained compartmentalization is an innate property of the digestive tract (Stainier, 2005).

In both structure and function, the *Drosophila* gut bears many similarities with the human gastrointestinal tract. It is divided into three discrete domains (foregut, midgut, hindgut) of different developmental origins (Demerec, 1950; Hakim et al., 2010). The foregut is of ectodermal origin and includes the pharynx, esophagus, and crop, an adult structure used to store food. A specialized structure, the cardia, is located at the foregut/midgut junction and functions as a sphincter to regulate food passage to the midgut. The midgut, one of the largest insect organs, is derived from the endoderm and is the main site of digestion and nutrient absorption. Finally, the hindgut is of ectodermal origin and is the major site of water reabsorption by concentrating excrement prior to elimination (Cognigni et al., 2011). Malpighian tubules, the functional analogs of the mammalian kidney, branch at the midhindgut junction (Demerec, 1950).

The adult *Drosophila* midgut consists of a simple epithelium, surrounded by visceral muscles, nerves, and trachea. The epithelium is renewed every 1–2 weeks through the activity of pluripotent ISCs (Micchelli and Perrimon, 2006; Ohlstein and Spradling, 2007). ISCs self-renew and give rise to enteroblasts, which gradually differentiate into either absorptive enterocytes

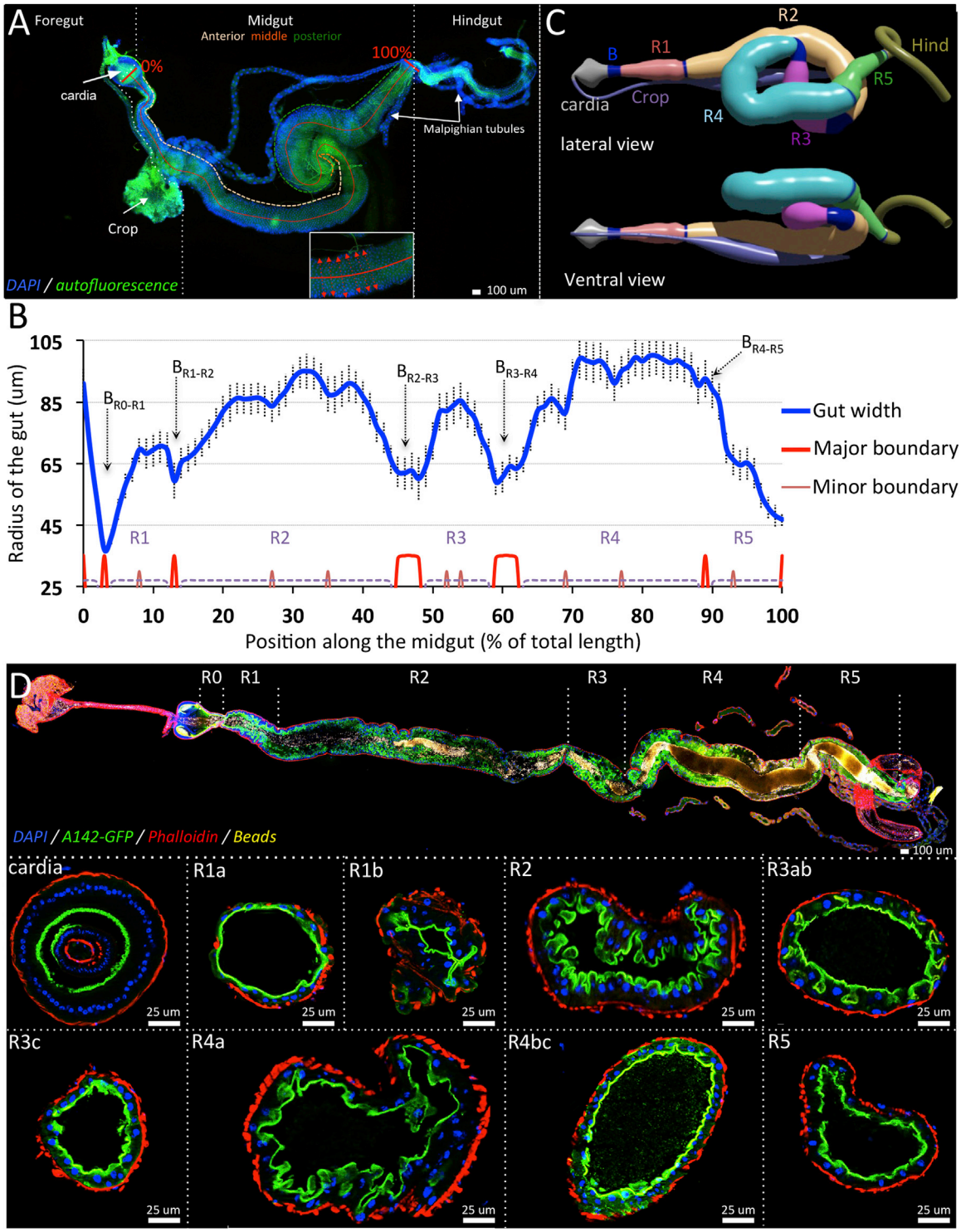

Figure 1. The Adult *Drosophila* Midgut Is Subdivided into Six Regions

(A) A representative picture of a dissected adult *Drosophila* gut stained with DAPI is shown. The gut is divided into three compartments: the foregut, midgut, and hindgut. Malpighian tubules run along the midgut and contact the gut together with the crop around B_{R1-R2}, at the thorax/abdomen junction. For measurements, we normalized the gut length to 100% starting from a position downstream the middle of the cardia (for more details, see Figure S1A) and ending at the midgut/hindgut junction. Green indicates autofluorescence.

(B) A morphometric analysis of the relative variations in the radius of the midgut of 5-day-old flies plotted along its length (%) revealed six major constrictions defining six regions. The curve represents the radius (with SE).

(legend continued on next page)

or secretory entero-endocrine cells. The adult midgut has been traditionally subdivided into three "segments": the anterior, middle, and posterior midgut. The middle midgut contains a pool of highly differentiated cells, the "copper cells," that are functionally related to the gastric parietal cells of vertebrates because they both secrete acid (Dubreuil, 2004). Although this coarse-grained compartmentalization of the midgut is well established, the existence of a more complex regionalization has been suggested in a number of observations. For example, several studies have shown that genes encoding some digestive enzymes, metal transporters, or antibacterial peptides are expressed in discrete parts of the gut (Abraham and Doane, 1978; Terra and Ferreira, 1994; Shanbhag and Tripathi, 2009; Wang et al., 2009; Buchon et al., 2009b). Moreover, a preliminary study analyzing the spatial expression of enhancer traps already suggested a complex subdivision of the larval gut into multiple compartments (Murakami et al., 1994). However, it is not entirely clear whether this regionalized gene expression is a consequence of different physiological states or rather reflects a regional identity. In this study, we present a comprehensive atlas of the morphological and functional properties of the *Drosophila* adult midgut regions and provide insights into the molecular mechanisms underlying their maintenance.

RESULTS

An Anatomical Atlas of Adult *Drosophila* Midgut Regions

We first generated an anatomical atlas of *Drosophila* midgut regions using a combination of morphometric and histological approaches. Because the midgut length is variable depending on the size of the fly and physiological context (length, 5.5 ± 1 mm), we normalized the gut length to 100% as measured from the center of the cardia and ending at the midgut/hindgut junction (Figures 1A and S1A). We found that the average midgut radius along the gut is not uniform (Figure 1B), revealing six major constrictions referred to as anatomical boundaries. In addition to the midgut layer embedded in the cardia (i.e., the region named R0 that was not analyzed in this study; see Figure S1A), these boundaries delimit five regions that were named R1–R5. Histological sections of whole flies revealed that the gut folds into a stereotypical 3D structure inside the abdominal cavity, which is schematized in Figure 1C. Projections of the five regions onto a 3D gut model showed that anatomical boundaries often correspond to inflexion points of the midgut in the abdomen, indicating a correlation between the 3D organization of the gut and its intestinal regionalization.

The first boundary, $B_{R0–R1}$, separates the endodermal part of the cardia from the anterior part of the midgut. The constriction site separating R1 and R2, $B_{R1–R2}$, corresponds to a particular anatomical "hub" at the frontier between the thorax and the abdomen, where both the crop and the Malpighian tubules interact physically with the midgut (Figures 1A and S1B). The two largest constrictions, $B_{R2–R3}$ and $B_{R3–R4}$, delineate the R3 compartment that corresponds to the copper cell region of the midgut. These two constrictions greatly reduce the lumen size and correspond to areas where the midgut abruptly folds and turns up (Figures 1C and S1C). Finally, the $B_{R4–R5}$ boundary precedes a region where the radius of the gut uniformly decreases as it turns up in the posterior body cavity to join the hindgut (Figures 1B and 1C). Two boundaries, $B_{R2–R3}$ and $B_{R3–R4}$, could be considered as microregions because they are composed of a range of enterocytes with distinct identities (Figure S1D; see Extended Results, Text S1, for details). Of note, six to eight muscle cells surrounding $B_{R2–R3}$ are the only gut cells expressing *Hand* (*Hand-Gal4 > UAS-GFP*, Figure S1E), which encodes a transcription factor (TF) involved in visceral mesoderm development and heartbeat contractions (Han et al., 2006; Popichenko et al., 2007).

To better characterize the fine-grained regional morphology along the midgut, we used conventional histological and immunological staining (Figures 1D and S2). This analysis revealed that three regions could be further divided into subregions based on different enterocyte architectures. In particular, the use of a transgene (*A142-GFP*) expressing a GFP fusion that localizes to the brush borders of enterocytes (Figure 1D) revealed that R1 could be further divided in two subregions including R1a, composed of flat cells, and R1b, composed of large folded enterocytes that greatly restrict luminal volume. In agreement with a previous study by Strand and Micchelli (2011), R3 could be subdivided into an anterior section containing copper cells (R3ab) and a posterior one (R3c) with large flat cells (LFCs). Finally, R4 could be subdivided in an anterior part (R4a), characterized by an extremely folded epithelium reminiscent of the villus of the mammalian intestine, and a posterior part (R4bc) composed of cells with short apical protrusions resulting in an enlarged lumen. Our morphometric analyses revealed the presence of smaller constrictions that probably delineate these subregions (Figure 1B). A more comprehensive description of the presented histological analysis can be found in a database that describes the major morphological features along the midgut (http://flygut.epfl.ch/histology).

Gene Expression Patterns Refine Midgut Regionalization

To further characterize the midgut epithelial compartments, we analyzed the expression patterns of 210 randomly selected reporter transgenes. These included 163 Gal4 enhancer and 47 GFP-protein trap lines whose expression reflects genomic enhancer activity. Of the 210 tested transgenes, 151 (72%) were expressed in the gut tissue, which is consistent with the FlyAtlas database that indicates that more than half of *Drosophila* genes are expressed in the adult midgut (Chintapalli et al., 2007). We excluded 59 reporter lines that were only expressed in small nucleated cells (including ISCs) from our study

(C) Lateral and ventral 3D representations of the *Drosophila* adult gut were generated using histological measurements. Midgut regions (marked with distinct colors) and boundaries (in blue) are indicated.

(D) Fluorescent confocal imaging (top lane) and histological sections (bottom panels) of a *Drosophila* gut. Green indicates brush borders (A142 GFP-trap). Blue presents nuclei (DAPI). Red illustrates visceral muscles (phalloidin). Yellow in the top panel corresponds to the bolus.

See also Figures S1 and S2.

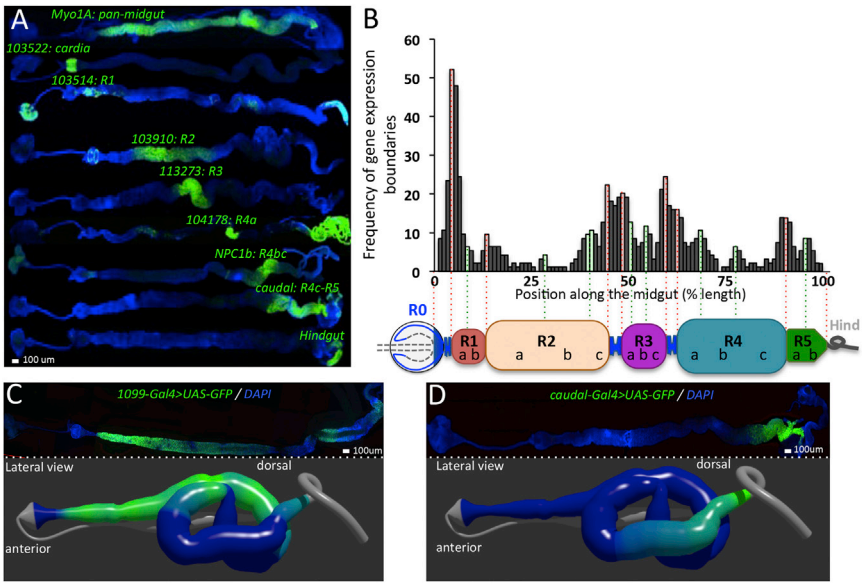

Figure 2. Gene Expression Patterns along the Midgut

(A) Expression patterns of a whole-gut (*Myo1A-Gal4*) marker as well as eight *pGal4* insertions that drive GFP in specific midgut regions. Genotype, *enhancerGal4 > UAS-GFP*.

(B) The graph displays the frequency of gene expression boundaries along the midgut. This graph derives from the analysis of 92 enhancer trap lines, yielding a total of 418 boundaries. The highest peaks (red dotted) correspond to the anatomical boundaries defined in Figure 1, whereas lower peaks (green dotted) mark the boundaries of subregions. A schematic model of midgut regions and subregions derived from anatomical and patterning studies is shown at the bottom. See Figure S3 and Extended Results for details.

(C) The *1099-Gal4* insertion drives GFP in three separate midgut regions that spatially cluster together at the dorsal level when projected onto the 3D gut model.

(D) Caudal (*Caudal-Gal4 > UAS-GFP*) is expressed following a gradient manner in R4 and R5a with highest levels at the midhindgut boundary.

because their expression was highly variable among individuals (http://flygut.epfl.ch/patterns). The expression of the remaining 92 transgenes was quantified by plotting the GFP signal intensity along the gut. All 92 transgenes are expressed in a patterned manner in enterocytes with the exception of seven lines that are ubiquitously expressed in the midgut (see examples in Figure 2A; the complete set of transgenes can be found at http://flygut.epfl.ch/patterns). The expression of 23 lines was confined to a single domain, whereas most others were expressed in a combination of domains.

We observed a high correlation between gene expression domains and the anatomical regions defined above. Specifically, we found several enhancer trap lines expressed in a unique region or subregion (Figure 2A). In addition, the expression of most transgenes switched on/off at discrete positions that correspond to the major anatomical boundaries defined above (Figures 2B and S3; Extended Results, Text S1). Although gene expression patterns are often variable, notably around the middle midgut, we found that their variation correlates with overall variations in gut morphology (Extended Results, Text S2; Figure S3E). In particular, these anatomical variations are mostly the result of the relaxed/contracted state of the visceral muscles surrounding the two boundaries, $B_{R2–R3}$ and $B_{R3–R4}$, that flank R3 (Figures S3F and S3G). The expression mapping of 92 transgenes not only validates the existence of the indicated regions and subregions (Figure 2B), but it also points to the presence of additional subregions that are devoid of obvious anatomical signatures. For instance, R2 could be further divided into three subdomains according to gene expression patterns (R2a, R2b, R2c). Collectively, the conjunction of our anatomical study with gene expression mapping suggests the existence of 14 distinct subregions grouped into 6 major regions, including R0 whose subdivision was not analyzed.

Except for few reporter transgenes that are specifically expressed in one region, most of the lines displayed complex expression patterns (Figure 2C). A large set of reporter transgenes (29%) is either expressed in the anterior and posterior part of the midgut but excluded from R3 or is exclusively expressed in R3. This confirms that the middle midgut forms a rather distinctive region of the midgut (Dubreuil, 2004; Shanbhag and Tripathi, 2009). About 15% of the enhancer trap lines showed a complex expression pattern involving three separate midgut domains. Upon projecting some of these complex patterns onto the 3D gut model, we observed that physically separated regions expressing a given transgene sometimes cluster together in 3D space (see Figure 2C for *1099-Gal4 > UAS-GFP*). Finally, 56% of reporter genes are expressed in a graded manner (Figure 2D). Most gradients occur in R1, R2, and R5, with a decreasing gradient from anterior to posterior along the midgut axis in R1 and R2, and an increasing gradient in R5. Interestingly, we noticed that all gradients start or stop at a boundary ($B_{prov–R1}$, $B_{R2–R3}$, and $B_{R5–Hindgut}$), suggesting a role for boundaries in mediating the organization of graded gene expression along the gut.

Establishment and Maintenance of Gene Expression Patterns

We next asked whether gene expression patterns along the midgut are stable, thus reflecting a regional identity, or whether they vary with the physiological state of the host. For this purpose, we compared the expression patterns of ten enhancer traps at different stages of the life cycle and in flies reared on different dietary regimes (Figures 3A and S4). Most transgenes are not "correctly" patterned immediately after eclosion, and their expression profile is established only after the first 2 days of adult life. Once established, patterns tend to remain stable in 5- to 8-day-old flies fed on different diets. Although the size of expression territories could be modulated by changes in the diet, no additional patterns were detected outside of their initial sites of expression (Figure 3B). However, we did observe

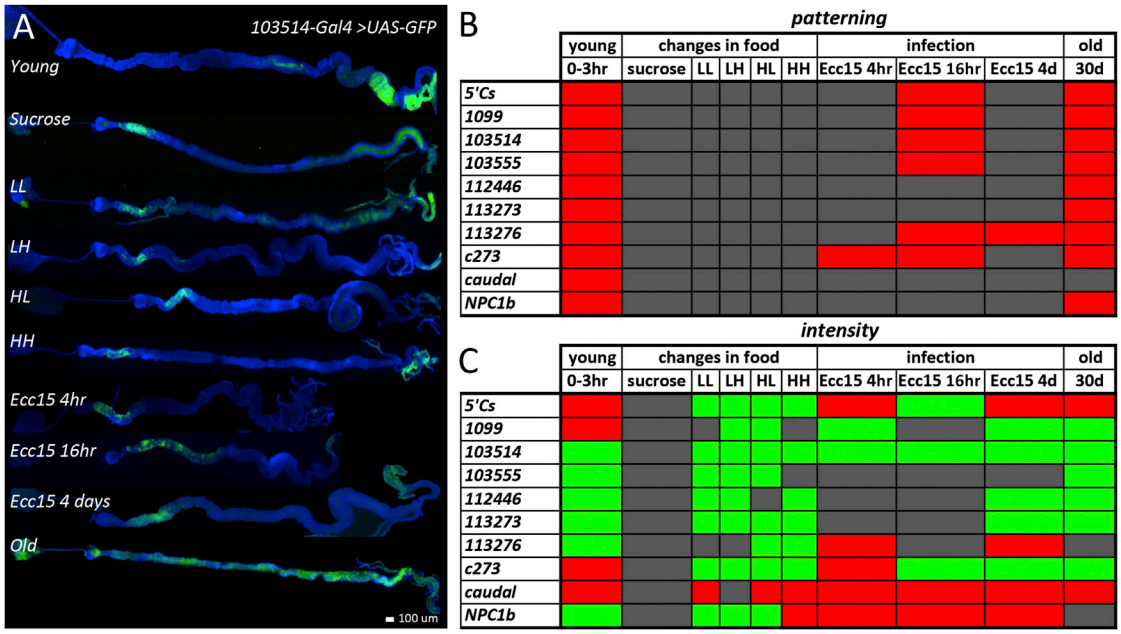

Figure 3. Dynamic Properties of Intestinal Gene Expression Patterns

(A) Representative expression patterns of the *103514-Gal4* insertion are shown for different conditions: young (3 hr posthatching) and old flies (30 days old), 5-day-old flies fed on different diets, and flies collected 4 and 16 hr after oral infection with *Ecc15*. The expression pattern remained specific to R1 excepted in young and old flies and in flies collected 16 hr postinfection. LL, low yeast, low sugar; LH, low yeast, high sugar; HL, high yeast, low sugar; HH, high yeast, high sugar.

(B and C) The experiment shown in (A) was performed for nine additional *pGal4* lines. Changes in gene expression patterns (B) are indicated in red, and changes in intensity levels (C) are indicated in red (increased signal) or green (decreased signal). A red color indicates a change in intensity compared to 5-day-old unchallenged flies on sucrose ($p = 0.05$). See Figure S4 for raw data.

changes in expression levels when the diet was altered (Figure 3C).

Previous studies have shown that the *Drosophila* midgut undergoes an age-related deterioration of the intestinal epithelium, which is associated with excessive ISC proliferation and aberrant enterocyte differentiation (Biteau et al., 2008; Choi et al., 2008). Accordingly, we found that 90% of intestinal gene expression patterns are altered in 30-day-old flies raised at 29°C. We then examined pattern stability in the midgut epithelium after an acute damage to the tissue. For this, the ten enhancer trap lines were fed with the pathogenic bacterium *Erwinia carotovora 15* (*Ecc15*), a challenge that induces the loss of half of the enterocytes and induces compensatory renewal of the intestinal epithelium (Buchon et al., 2009a). Interestingly, we found that the expression territories of seven of the ten reporter transgenes were altered 16 hr after ingestion of *Ecc15*, although the original wild-type pattern was restored 4 days postinfection (Figure 3B).

Transcriptome Analysis of the Main Gut Domains

To gain insights into the functional compartmentalization of the intestine, we monitored transcriptome variations in gut regions. In addition to the five main midgut regions defined above, we dissected the crop and the hindgut of 5- to 8-day-old $Oregon^R$ flies and performed Affymetrix microarray analyses. We found that about 62% of the *Drosophila* genes are expressed at detectable levels in at least one gut region, which is consistent with the FlyAtlas database (Chintapalli et al., 2007) (statistical analyses and full data set can be found at http://flygut.epfl.ch/expressions). Among them, 1,500 genes can be considered as "region markers" because they are enriched in only one region. We validated 46 of these genes by quantitative RT-PCR (qRT-PCR) experiments using independent, region-specific RNA extracts (Figure S5A). A comparison with the FlyAtlas database (Chintapalli et al., 2007) revealed that 40% of these genes are expressed specifically in the gut (Figure S5B), confirming that some of these markers are both gut and region specific. Clustering of the microarray data revealed a clear dichotomy between regions of ectodermal versus endodermal origin as well as similarities in gene expression profiles of midgut regions, especially between regions R2 and R4 (Figure S5C). To characterize the function of each region, we performed a Gene Ontology (GO) analysis on the genes enriched in each region (Figures 4A and 4B). This analysis indicates a functional specialization of the different gut regions (detailed in Extended Results, Text S3). In particular, digestive enzymes, immune genes, or genes encoding components of the mucus and the peritrophic matrix (a chitinous layer lining the midgut epithelium) showed differential enrichment along the gut (examples in Figure 4B). Of note, transcripts encoding enzymes involved in the processing of complex macromolecules are enriched in the anterior part of the gut (especially in R2), whereas those involved in the processing of simpler nutrients are more abundant in R4. This could reflect the sequential breakdown and absorption of food along the gut. In addition, our analysis revealed that many digestive genes that are organized in large genomic clusters are sequentially expressed in different gut regions. For instance, each of the 11 *Trypsin* genes

A

			Crop	Cardia/R1	R2	R3	R4	R5	Hindgut
DEFENSE RESPONSE	Immunity	Pathways	Toll	Imd					Toll
		Others	Melanisation, Teps, Lysozymes, Duox						Duox
	Abiotic stress	Redox	+++						++
		Detoxification	+++						+
GUT STRUCTURE	Cuticle Peritrophic matrix	Chitin binding	++	+++					++
		Mucus	+	++					
		Cuticular proteins	+++	+					+
METABOLISM	Protein metabolism		Serpin L serine biosynthesis		Serine peptidase		Serine peptidase	Serine peptidase	Serpin
	Lipid metabolism		Acylglycerol and Steroid metabolism	Very long chain fatty acid metabolism	Triglycerides lipase Fatty acid oxidation LDL binding	Thiolester Hydrolase Acylglycerol metabolism	Triglycerides lipase Sphingolipid metabolism Pantetheine hydrolase Ceramidase activity Fatty acid oxidation Sterol binding	Acylglycerol metabolism	
	Carbohydrates metabolism				Complex carbohydrates		Complex and simple carbohydrates		Glycogen biosynthesis
	Vitamin metabolism		++	++			+++		
	Transport	Symporter		Hydrogen-Sugar	Solute-Cation Sodium-Phosphate				
		Others		Amino acid Sugar	Cholesterol Water channel Sodium Amino acid	Solute-solute antiporter Metal Hydrogen	Cholesterol Active transmembrane transporter	Sodium L amino acid	Calcium Organic cation Ammonium
	Diverse		Alcohol catabolism					Zinc ion Binding Glucuronosyl-transferase activity	

B

	Functions	Genes	Crop	cardia/R1	R2	R3	R4	R5	Hindgut
METABOLISM	Vitamin metabolism	Cralbp	4.33	7.63	-8.36	-7.4	-5.93	-7.52	-8.09
	Sugar transport	sut2	-6.3	6.29	-2.37	-4.84	-2.72	-2.72	-4.82
	Serine peptidase	CG7542	-450.91	-23.66	1.72	-6.72	-7.79	-80.68	-746.75
	Serine peptidase	Jon25Bi	-110.95	-1.1	1.13	-10.15	-4.76	-29.53	-177.42
	Glucosidase	CG8690	-52.9	-1.07	3.46	-3.34	-2.23	-21.62	-57.3
	Lipoprot. transport	LpR1	-9.03	-5.21	3.9	-6.81	-2.64	-13.79	-9.34
	Aquaporin	CG17664	-5.97	-3.77	2.42	-4.72	1.16	-2.63	-7.93
	Antiporters	CG8177	-8.49	-2.28	-6.75	20.08	-5.47	-1.36	-1.14
	Metal transport	ZnT63C	-1.15	-1.03	1.5	3.36	1.09	-1.02	-1.02
	Serine peptidase	Jon44E	-326.03	-254.5	-39.02	-8.66	2.03	-35.36	-357.35
	Amylase	Amyd/Amy-p	-156.24	1.09	1.01	-4.18	1.02	-19.93	-311.49
	glucosidase	LvpL	-136.52	-119.21	-16.08	-31.91	2.73	-1.74	-69.78
	Ceramidase	CDase	-14.02	-15.9	-4.02	-8.53	2.7	-1.98	-69.42
	Triglyceride lipase	CG2772	-79.25	-98.38	-40.68	-63.49	3.07	-3.29	-74.72
	Sterol esterase	mag	-139.11	-197.37	-18.6	-1.99	2.08	-24.32	-152.93
	Cholesterol metabolism	ACAT	-18.69	-12.74	-7.02	-8.31	2.73	1.14	-8.08
	Lipid binding	Npc2c	-23.35	-23.01	-15.4	-18.69	2.53	-1.91	-24.54
	Sterol metabolism	ScpX	2.68	-1.55	-1.87	-2.65	2.06	-1.71	-2.64
	Chymotrypsin	CG31267	-61.57	-74.19	-52.07	-29.49	-16.1	8.19	-2.66
	Chymotrypsin	CG4053	-68.49	-64.59	-34.02	-40.03	-1.23	7.59	-21.09
	Glucuronosyltransferase	Ugt86Dh	-30.23	-2.87	-1.61	1.14	1.63	3.7	-5.41
	Ammonium transport	Rh50	-3.24	-2.94	-6.05	-5.52	-4.37	-3.9	30.83

<-10 <-6 <-2 >2 >4 >6 >8 >10

	Functions	Genes	Crop	cardia/R1	R2	R3	R4	R5	Hindgut
GUT STRUCTURE	PM constituent	Muc68D	-113.25	10.78	-49.45	-98.07	-74.88	-35.6	-142.66
		Peritrop-A	-1.21	3.7	-1.52	-1.57	-1.5	-1.56	-1.25
		Cry	-23.09	-31.55	-8.59	-4.86	2.62	-1.02	-36.84
		CG17145	-3.02	-2.11	-1.75	-2.66	2.39	-2.08	-2.51
	Chitin binding	pot	16.07	3.89	-2.24	-1.63	-2.57	-1.07	8.53
	Chitinase	Cht8	-57.02	7.38	-40.2	-63.06	-26.94	-47.42	-85.73
DEFENSE RESPONSE	ROS burst	Duox	2.71	1.84	-1.01	1.01	-1.06	-1.03	2.12
	Toll pathway	spz	12.43	3.61	-1.5	-1.43	-1.5	-1.22	9.93
		Drs	5.82	-3.02	-3.56	-6.22	-7.19	-4.67	1.56
		PGRP-SA	9.16	-1.01	-1.23	-1.57	-1.54	-1.3	2.66
	Melanisation	Spn27A	23.01	2.58	-3.14	-2.9	-3.17	-2.48	1.73
	Gram- recognition	PGRP-LC	3.2	1.19	-1.01	1.06	-1.25	1.22	5.78
		PGRP-LE	-1.42	1.29	1.22	2.07	1.45	1.21	-1.5
	Imd negative regulators	pirk	2.07	-2.51	-1.36	1.31	1.22	-1.08	1.19
		PGRP-LB	1.54	-2.79	-1.32	2.9	1.39	-1.83	-6.19
		PGRP-SC1	-123.07	-121.98	-31.68	-5.46	2.24	-27.07	-133.13
	AMPs	Def	-3.91	8.05	-12.31	-13.24	-9.84	-13.28	-13.43
		DptB	1.17	4.19	-3.84	-4.74	-3.79	-3.34	-1.11
		Dro3	-13.16	1.57	-1.01	-1.02	1.08	-7.46	-12.27
	ROS stress	GstE2	2.33	1.09	1.12	-1.08	-1.12	1.69	1.3
	Detoxification	Cyp312a1	33.31	-1.01	-2	-1.81	-2.03	-1.72	2.55
		Cyp4e3	11.78	-1.33	-1.32	-1.55	-1.28	1	1.16

C

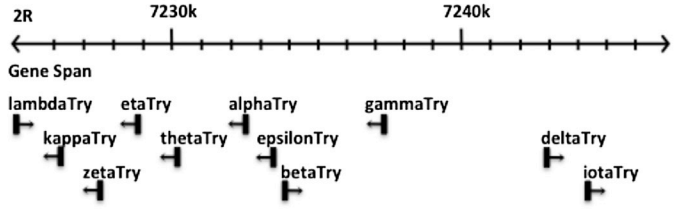

D

	Crop	cardia/R1	R2	R3	R4	R5	Hindgut
delta/ gammaTry	-411.99	1.09	1.34	-1.91	-1.21	-28.98	-344.97
alphaTry	-104.59	-1.07	1.02	-1.26	-1.68	-3.5	-35.9
betaTry	-117.53	-1.03	1.05	-3.58	-3.33	-9.11	-272.31
epsilonTry	-179.75	-1.09	1.11	-5.48	-8.55	-26.07	-415.34
thetaTry	-114.26	-26.35	1.14	1.9	-1.52	-39.39	-129.3
kappaTry	-198.79	-1.76	-1.78	-9.09	2.1	-1.17	-135.47
lambdaTry	-161.46	-76.23	-11.29	-22.52	1.97	-1.59	-199.23
iotaTry	-122	-133.52	-23.96	-63.91	2.51	1.8	-32.24
etaTry	-110.54	-3.4	-2.9	-13.03	1.96	2.68	-20.33
zetaTry	-109.86	-303.88	-89.05	-87.17	1.77	2.96	-8.23

(legend on next page)

that form a cluster at the cytological site 45A is specifically expressed in a subset of regions (Figures 4C and 4D). This feature appears common to other clusters including Jonah proteases, α-esterases, mannosidases, and lipases (data not shown). An exception to this rule is a cluster of chymotrypsins at cytological position 89F1, which are all enriched only in R5. Collectively, our study indicates that each region forms a specialized functional unit, containing enterocytes with a peculiar shape and expressing a distinct gene repertoire.

Multiple TFs Mediate Midgut Compartmentalization

Our analysis implies the existence of complex gene regulatory networks that control the functional stratification of the gut. However, the structural and dynamic properties of these regulatory networks are largely unknown. Our microarray data set and the FlyAtlas database (Chintapalli et al., 2007) indicated that around 460 TFs are expressed in the gut out of the ~750 encoded in the fly genome. This high number probably reflects the complexity of this organ, which comprises several cell types including stem cells, enterocytes, entero-endocrine cells, trachea, neurons, and visceral muscles. We found that the genes encoding most TFs associated with signaling pathways usually involved in (i) development (EGFR: *pointed*; Notch: *Su(H)*; JAK-STAT: *Stat92E*; Wnt: *pangolin*; Dpp: *Mad*; hedgehog: *Cubitus interruptus*), (ii) immunity (imd: *Rel*; Toll: *dif*), (iii) growth (hippo: *Yorkie*, *Scalloped*; Insulin: *foxo*), and (iv) stress (JNK: *kayak*; Keap: Nrf2) are expressed in the gut. Of the 460 TFs, 52 are expressed in a patterned manner along the gut, showing at least a 2-fold enrichment in one specific region compared to the entire gut. Among them, 11 TFs are exclusively enriched in one region suggesting a role in local gut regionalization (Figure 5A; data not shown).

We hypothesized that gut compartmentalization could be mediated by general tissue identity cues provided by "pan-midgut" TFs and be further refined by local cues provided by "region-specific" TFs. To test this hypothesis, we analyzed the function of ten TFs that were selected based on their exclusive expression in one region (*Tango*, *Ptx1*, *labial*, *CG34376*, *caudal*, *CG3242*) or their enrichment in the gut compared to other organs (*GATAs*, *Bigmax*) (Figure 5A). We knocked down the expression of these ten TFs by *RNAi* in enterocytes using a temperature-sensitive Gal4 construct (*Myo1A-Gal4^{ts} > UAS-TF-IR*). To circumvent possible developmental effects, RNAi expression was induced at 3 days posteclosion (i.e., after the patterning of the gut is fully established), and guts were dissected 7 days later. We then investigated the role of these TFs in the functional regionalization of the gut by monitoring their impact on the expression of 40 region marker genes. Figure 5B shows that depletion of almost all of the tested TFs affected expression of some of these marker genes. Although TFs that are expressed all along the midgut (*Bigmax*, *GATAe*) tended to affect the expression of most markers, region-specific TFs had more localized effects (Figure 5B and text below). Contrary to this trend, silencing of *caudal* and *CG34276*, which encode, respectively, a homeobox TF enriched in the posterior midgut and an unknown TF specific to R4, resulted in a broad derepression of intestinal markers, even of genes normally restricted to the anterior midgut. These results indicate that a complex, hierarchical network of TFs mediates regional identity along the intestine.

Maintenance of Gut Regionalization in Adults Requires TFs Involved in Midgut Development

Several TFs expressed in the adult midgut, notably *GATAe* and the homeobox *labial*, were initially characterized for their role in gut development (Hoppler and Bienz, 1994; Dubreuil et al., 1998; Okumura et al., 2005). This suggests that genes involved in gut differentiation during development also participate in the maintenance of intestinal regionalization at the adult stage. To test this hypothesis, we analyzed the regulatory roles of *GATAe* and *labial* in the adult midgut in further detail.

Using the brush border GFP marker A142, we found that *GATAe* is required for enterocyte morphological identity because silencing of *GATAe* (*Myo1A-Gal4^{ts} > UAS-GATAe-IR*) disrupted the shape of enterocytes with the strongest effect observed in the anterior part of the midgut (Figure 5C). In addition, qRT-PCR experiments revealed that *GATAe* is required for the expression of most genes in the midgut, including those encoding digestive enzymes (Figures 5B–5E). In contrast, silencing of *GATAd* by *RNAi* did not produce any major effect on gene expression or intestinal structure despite the fact that this TF is also enriched in the adult midgut (Figures 5C–5E). Finally, we found that the rate of food transit was defective in the *GATAe* (Figure 5D), thus revealing a critical role of *GATAe* in maintaining adult midgut homeostasis by controlling directly or indirectly both enterocyte structure and digestive function.

The *Hox* gene *labial* is required for the development of copper cells at the embryonic stage and their maintenance in larvae (Hoppler and Bienz, 1994; Dubreuil et al., 2001). In adults, *labial* is specifically expressed in the R3 region, which contains copper cells (Figure 5A). We therefore investigated its role in the maintenance of R3 identity. Silencing of *labial* in enterocytes of adults (*Myo1A-Gal4^{ts} > UAS-lab-IR*) resulted in the loss of invaginated cells, characteristic of copper cells, within 10 days (Figure 6A). The remaining R3 enterocytes of *labial* RNAi midguts displayed a smoothed shape reminiscent of enterocytes found in R2 or R4. Moreover, *labial* knockdown impaired the expression of a subset of the R3-specific genes, including those encoding the serine protease Jon65Aii, the peritrophic matrix component Drosocrystallin, and the uncharacterized gene *CG5770* (Figure 6B). Another homeobox-like gene, *Ptx1*, is strongly enriched

Figure 4. Transcriptome Variations in Gut Regions

(A) This table shows a selection of functional categories identified by GO analysis of genes that are enriched by at least 2-fold in a region. The number of "+'" reflects the extent of gene enrichment for a specific GO category.

(B) A selection of 44 genes upregulated in specific gut regions. Functions, names, and fold enrichment (compared to whole gut) are indicated.

(C and D) A total of 11 trypsin genes are clustered together on chromosome II (C). The expression of each gene of this cluster is enriched in different regions (D). The microarray was performed on gut fragments corresponding to the crop, cardia/R1, R2–R5, and the hindgut.

See also Figure S5 and Extended Results.

A

Genes	Crop	Prov/R1	R2	R3	R4	R5	Hindgut
Bigmax	1.32	-1.96	-1.68	-1.09	1.85	1.93	-1.53
pangolin	1.24	-1.03	1	-1.08	1.1	1.09	1.03
GATAe	-21.82	1.34	1.56	1.42	1.56	1.49	-6.6
GATAd	1.66	2.54	1.3	2.7	1.17	2.44	2.86
tango	3.11	1.97	1.07	3.02	-1.05	1.73	2.7

Genes	Crop	Prov/R1	R2	R3	R4	R5	Hindgut
Ptx1	-6.83	-9.02	-1.22	10.55	-1.14	-4.1	-7.51
Labial	-5.24	-4.12	-3.36	23.38	-4.31	-5.1	-4.93
CG34376	-7.57	-1.19	1.72	-4.02	2.62	-2.07	-4.54
Caudal	-7.27	-20.08	-17.08	-4.14	1.92	4.44	-2.04
CG3242	-2.23	1.37	1.87	-2.07	-1.91	5.28	1.06

<-10 <-6 <-2 >2 >4 >6 >8 >10

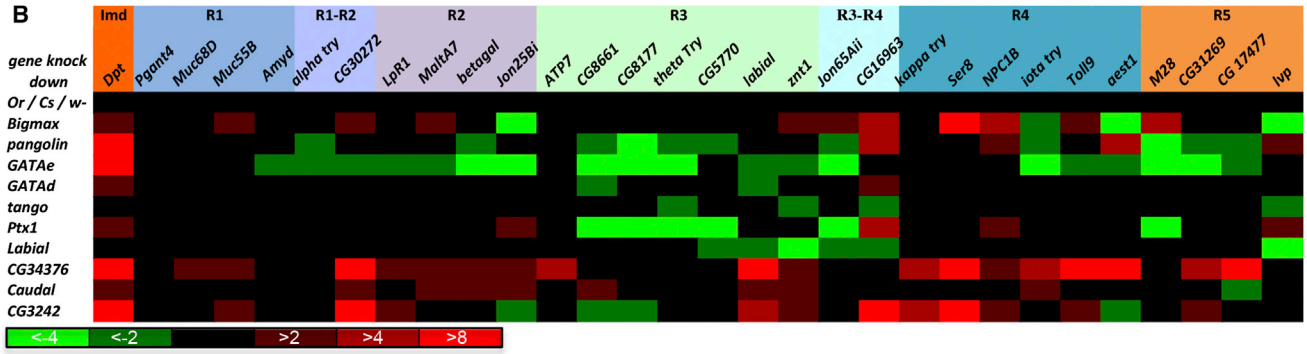

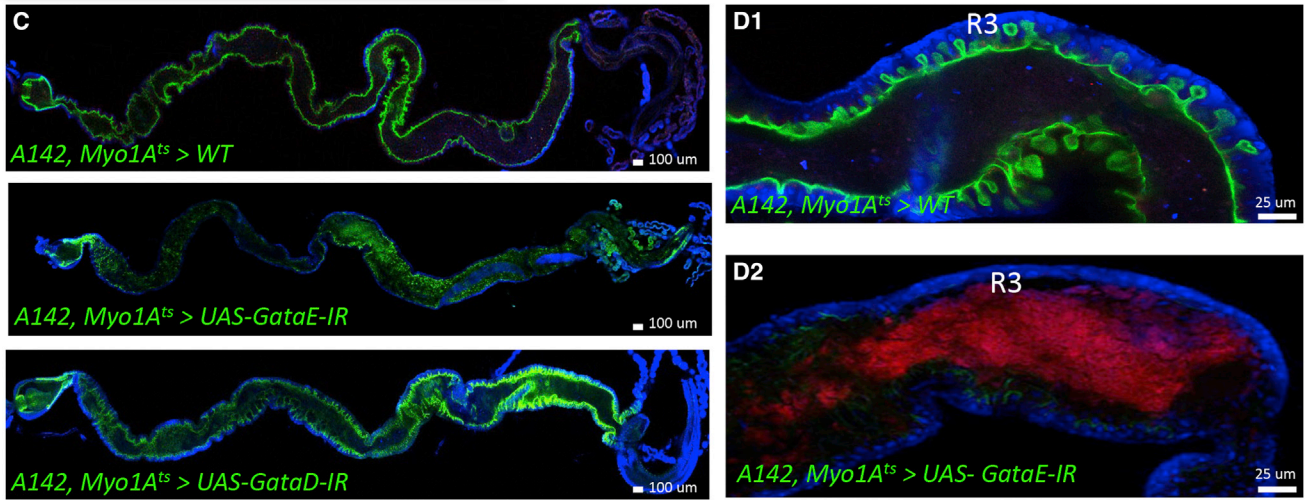

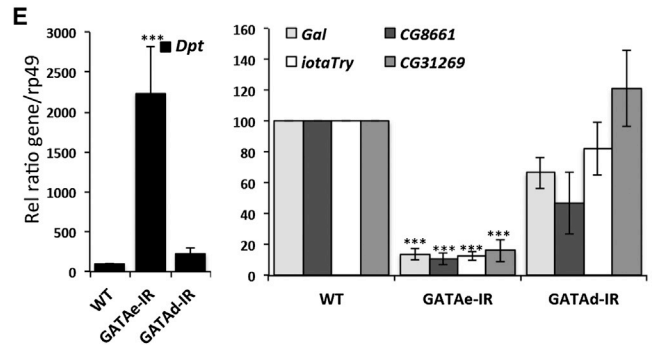

Figure 5. A Combination of TFs Regulates Midgut Regionalization

(A) Gene expression enrichment of ten TFs along the gut as revealed by the microarray analysis. *Bigmax*, *GATAd*, and *GATAe* are expressed all along the midgut, whereas *tango*, *Ptx1*, *labial*, *CG34376*, and *Caudal* are expressed in specific regions. Values indicate the fold enrichment in gene expression for each region compared to the entire gut.

(B) The expression of 30 region-specific genes was assessed by qRT-PCR in the midgut of wild-type flies or flies in which the expression of a given TF was reduced by RNAi (genotype, *Myo1A-Gal4^{ts} > UAS-TF-RNAi*). The intensity of the red or green indicates, respectively, the level of up- or downregulation when the TF was knocked down (fold change compared to wild-type). Black indicates no change.

(legend continued on next page)

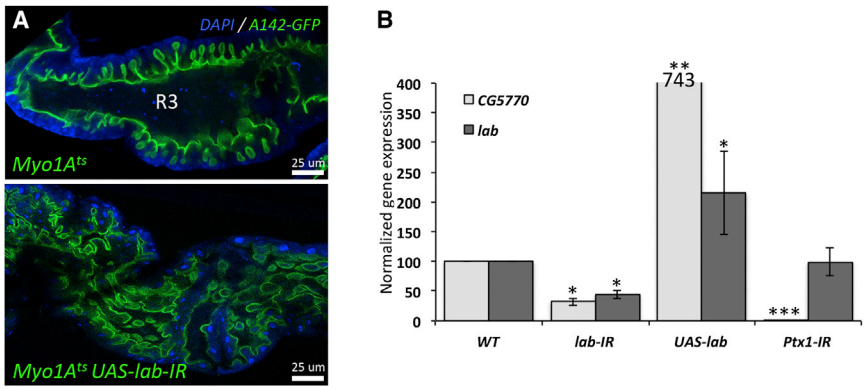

Figure 6. The Homeobox Genes *labial* and *Ptx1* Control the R3 Region

(A) Fly guts with reduced *labial* expression in enterocytes (*Myo1A-Gal4^{ts}* > *UAS-lab-IR*) display a loss of copper cells in R3 as illustrated by the loss of ring-shaped brush borders.

(B) Expression of the R3-specific gene, *CG5770*, requires both *labial* and *Ptx1* as revealed by qRT-PCR. These experiments were performed on whole-gut extracts derived from wild-type flies, flies with reduced *Ptx1* or *labial* expression (*Myo1A-Gal4^{ts}* > *UAS-lab-IR and Myo1A-Gal4^{ts}* > *UAS-Ptx1-IR*), or overexpressing labial *(Myo1A-Gal4^{ts}* > *UAS-lab*). This figure also shows that *labial* expression was efficiently reduced in *Myo1A-Gal4^{ts}* > *UAS-lab-IR* flies. Data are mean ± SEM of at least three repeats. *p < 0.05, **p < 0.01, and ***p < 0.001, Student's t test.

in R3 (Figure 5A). Knockdown of *Ptx1* by RNAi (*Myo1A-Gal4^{ts}* > *UAS-Ptx1-IR*) at the adult stage abrogated the expression of the three R3 gene markers (*CG8661*, *CG8177*, *thetaTry*) that were not affected by the depletion of *labial*. Interestingly, the expression of *CG5770* required both *labial* and *Ptx1*, suggesting a cooperative effect of both TFs in the control of R3-specific genes (Figure 6B). Our results indicate that TFs involved in the specification and differentiation of the gut during development are also required to maintain the functional regionalization of this organ at the adult stage.

Graded Activity of the Wnt Pathway in the Adult Midgut

Our study shows that many transgenes are expressed in gradients in the vicinity of intestinal boundaries. This suggests the existence of regulatory mechanisms in the gut that can spatially organize gene expression according to their distance to an anatomical boundary. The Wnt signaling pathway regulates ISC behavior in both mammals and *Drosophila* (Lin et al., 2008; Schuijers and Clevers, 2012). This pathway is also involved in the generation of many developmental gradients in response to Wingless, a Wnt ligand. This prompted us to investigate a possible role of the Wnt pathway in establishing graded gene expression patterns in the adult midgut. To monitor Wnt pathway activity in further detail, we analyzed the expression pattern of *Fz3-RFP*, a Wingless-responsive reporter transgene (Figures 7A and 7B) (Olson et al., 2011). Consistent with a previous study by Cordero et al. (2012), *Fz3-RFP* was found to be expressed in ISCs (Figures 7B and S6A). Interestingly, *Fz3-RFP* was also strongly expressed in enterocytes at three distinct sites of the midgut: around R1a, R2c, and R5, and weakly around R4a (Figure 7C). The quantification of *Fz3-RFP* signals revealed that *Fz3-RFP* exhibits four intensity gradients, all culminating at a boundary ($B_{prov–R1}$, $B_{R2–R3}$, $B_{R3–R4}$, $B_{R5–Hindgut}$; Figure 7C). Remarkably, the gradient of *Fz3-RFP* overlaps with the gene expression gradients previously identified with Gal4 enhancer trap lines (similar orientation for R1 and R5, opposite for R2c; Figures 7C and S6B). In addition, the morphology of enterocytes of $B_{R2–R3}$ gradually changes following the *Fz3-RFP* gradient (Figure S6C). This suggests that the Wnt pathway activity could influence both gene expression and enterocyte architecture at the vicinity of boundaries. Knockdown of *pangolin* by RNAi or with a dominant-negative form (*Myo1A-Gal4^{ts}* > *UAS-pan-IR* and *Myo1A-Gal4^{ts}* > *UAS-pan^{DN}*) revealed a role for this TF in the regulation of genes expressed in R3 and R5 (such as the peptidase gene *M28*), where *Fz3-RFP* activity is maximal (Figures 5B and 7D). These results were confirmed by overexpressing either the Wnt pathway inhibitor Shaggy or the Wnt pathway activator Armadillo (*Myo1A-Gal4^{ts}* > *UAS-sgg*, *Myo1A-Gal4^{ts}* > *UAS-armadillo^{S10}*; Figure 7D). To test whether the graded activity of the Wnt pathway could be responsible for some of the gene expression patterns in gradients, we monitored the effect of expressing a dominant-negative form of *pangolin* on the expression pattern of the *113276-Gal4* transgene, which drives Gal4 in a graded manner in the R5 region. Figure 7E shows that *pangolin* is required for the expression of *113276-Gal4* in R5. In addition, the *113276-Gal4* expression pattern expanded upon Wingless overexpression (genotype: *113276-Gal4* > *UAS-wg, UAS-GFP*, Figure S6D). Altogether, our results suggest a role for the Wnt pathway in organizing gene expression in the vicinity of gut boundaries.

TFs that Regulate Gut Compartmentalization Maintain Its Homeostasis

Knockdown of the homeobox gene *caudal* leads to the direct derepression of antimicrobial peptide genes in the gut, a situation reminiscent of inflammatory bowel disease in humans (Ryu et al.,

(C) Silencing *GATAe* but not *GATAd* affects enterocyte morphology mainly in the anterior midgut as revealed by the brush border marker *A142-GFP*. Genotypes are indicated in the figures.

(D1 and D2) A higher magnification of the R3 region shows that knocking down *GATAe* results in a disruption of brush border morphology (as well as in the accumulation of food [in red] due to an intestinal occlusion). DAPI is in blue.

(E) qRT-PCR on gut RNA extracts of 7-day-old flies revealed that the antibacterial peptide *Diptericin* (*Dpt*) is upregulated in midguts upon reduced *GATAe* expression (*Myo1A-Gal4^{ts}* > *UAS-GATAe-IR*). Knockdown of *GATAe*, but not *GATAd*, alters the expression of digestive enzymes (*β-Galactosidase*, *iota trypsin*, *CG31269*) and the R3 marker gene *CG8661*. Data are mean ± SEM of at least three repeats. ***p < 0.001, Student's t test.

See also Figure S7.

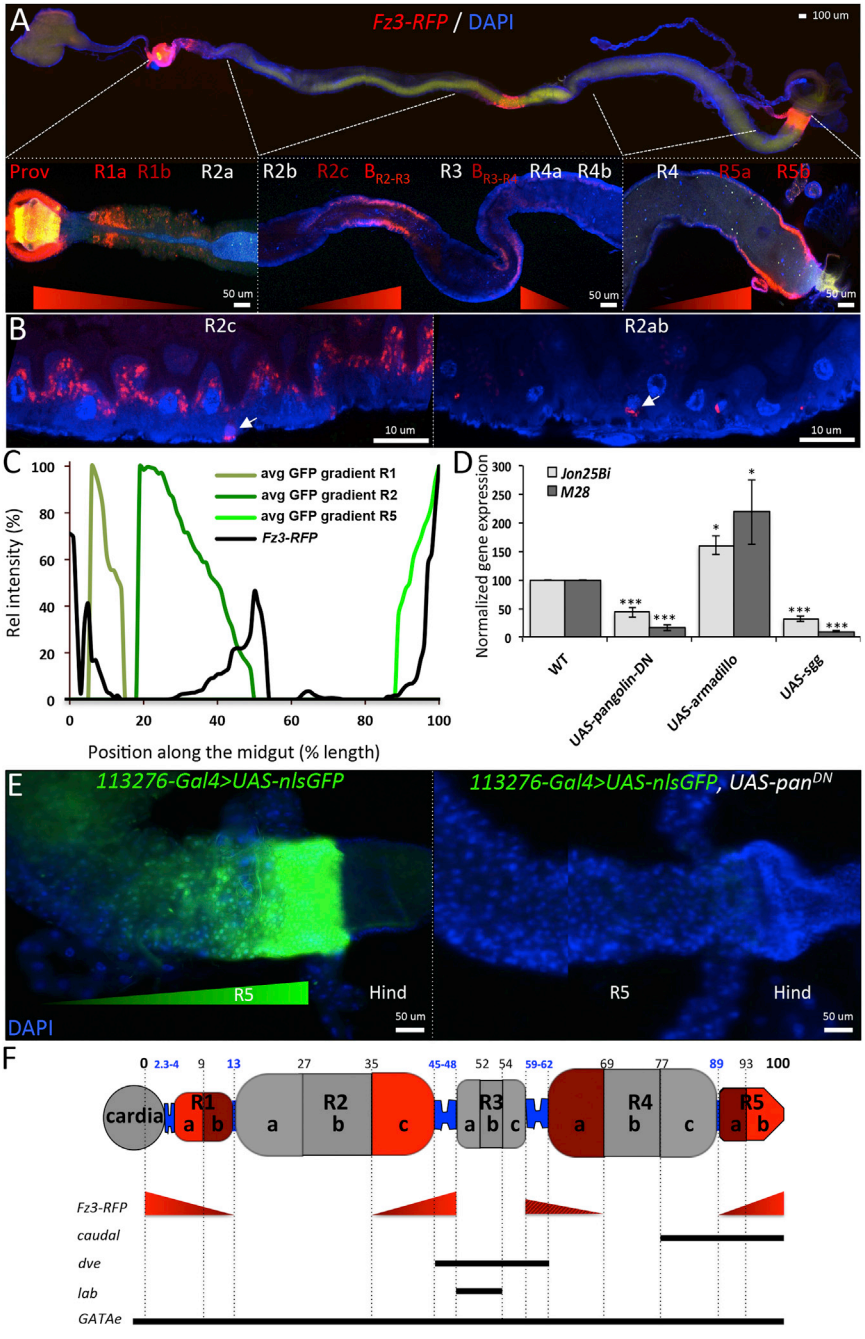

Figure 7. The Wnt Pathway Exhibits a Graded Activity around Intestinal Boundaries

(A) The expression pattern of *Fz3-RFP*, a reporter gene for Wnt pathway activity, revealed that this pathway is activated in a graded manner in enterocytes of R1, R2c, R4a, and R5 (the lower panels show higher magnifications of the four different gradients). In R4a, the expression of *Fz3-RFP* was weaker and more variable from one fly to another.

(B) Higher magnification shows that *Fz3-RFP* is detected in ISCs (white arrows) and in enterocytes located in the vicinity of boundaries.

(C) Quantification of *Fz3-RFP* signal along the midgut was compared to the average (avg) expression level of 56 Gal4 lines yielding graded expression. The gradients of Wnt pathway activity follow a similar (R1 and R5) or an opposite (R2c) direction compared to those exhibited by the *pGal4* insertions. Rel, relative.

(D) The expression of the R2–R3 (*Jon25Bi*) or R5 (*M28*) region-specific genes is altered in flies with reduced (*Myo1A-Gal4^{ts} > UAS-pan^{DN}; Myo1A-Gal4^{ts} > UAS-sgg*) or increased (*Myo1A-Gal4^{ts} > UAS-armadillo^{S10}*) Wnt pathway activity in enterocytes as revealed by qRT-PCR of whole guts. Data are mean ± SEM of at least three repeats. *$p < 0.05$ and ***$p < 0.001$, Student's t test.

(E) The*113276-Gal4* insertion expresses GFP in a graded manner in R5 of 5-day-old wild-type flies, but not in flies expressing a dominant-negative form of *Pangolin* in enterocytes.

(F) Schematic representation of the gut illustrating the expression pattern of *Fz3-RFP* as well as those of the TFs discussed in this paper. The organization of the midgut shows an overall symmetry centered on R3.

See also Figure S6.

2008). We investigated whether this immune disorder was specific to *caudal* mis-expression or whether other TFs involved in gut compartmentalization could also impact intestinal homeostasis. Intriguingly, we found that silencing eight out of the ten TFs we tested resulted in an upregulation of the Imd pathway, as revealed by the high expression of the antibacterial gene *Diptericin* (Figure 5B). This suggests that a general consequence of the loss of normal gut compartmentalization is an increased stress on the gut linked to immune activation. Stresses that damage the gut are generally associated with an increase in stem cell division to compensate for the loss of enterocytes (Amcheslavsky et al., 2009; Jiang et al., 2009; Buchon et al., 2009b). Consistent with these observations, we observed an increase in the number of ISCs undergoing mitosis in the guts of most TF *RNAi* flies, including *caudal*, *Pangolin*, and *labial* (Figure S7A). Furthermore, flies with reduced TF expression in enterocytes have shorter lifespans in both unchallenged and infectious conditions (Figure S7B; data not shown for *Ecc15* infection). Taken together, these data indicate that the disruption of TFs involved in midgut compartmentalization affects the overall function of the alimentary canal and leads to intestinal disorders that compromise the animal's fitness. See Extended Results for more information.

DISCUSSION

The Midgut Is Comprised of Six Morpho-Functionally Distinct Regions

The midgut has previously been divided into three regions based on the presence of acid-secreting cells in the adult middle

midgut (Dimitriadis, 1991). Our morphometric, histological, and genetic analysis leads us to propose a subdivision of this organ into six major regions that are themselves divided in subregions. Each of the six major regions is delimited by boundaries that mark (1) an anatomical constriction, (2) a change in tissue histology, and (3) a site where gene expression patterns change at high frequency. In addition, we further divided regions R1–R5 into 14 subregions, which are only defined by histological and/or gene expression pattern change. Although the existence of the six major regions is overt, we cannot completely rule out further refinement of these regions beyond the 14 that we have identified in this study. Interestingly, the observation that gene expression patterns along the gut correlate with anatomical and histological features reinforces our model of midgut compartmentalization.

Our study also shows that major regions are separated by anatomical boundaries that correspond to points of inflection where the midgut folds stereotypically inside the body cavity. It should be noted that two boundaries, $B_{R2–R3}$ and $B_{R3–R4}$, could be considered as distinct microregions because they are composed of enterocytes and muscle cells with specific identities. It is probable that these two boundaries act as sphincters to regulate food transit because they correspond to points of constriction of the intestinal lumen and contain muscles with specific identify. A recent study has shown that the *Drosophila* intestine is innervated by sensory and efferent fibers confined to three discrete portions along the digestive tract (Cognigni et al., 2011). This pattern of innervation correlates with region boundaries (see Figure S1F), thereby giving credit to our model of gut compartmentalization. Collectively, our study provides comprehensive insights into *Drosophila* adult midgut organization, revealing an underlying complexity that was hitherto not appreciated. The regionalization of the midgut should be taken into consideration in future studies addressing questions related to ISCs, immunity, and gut metabolism.

Organization of the *Drosophila* Gut into Discrete Functional Units

Optimization of nutrient uptake requires the diversification and adaptation of regions of the gastrointestinal tract to deal with food at different stages of digestion (Karasov et al., 2011). Our microarray analysis provides a glimpse into the functional diversification of *Drosophila* gut regions. The sequential processing of food is highlighted by the enrichment in enzymes degrading macromolecules in the anterior part of the gut, whereas posterior segments are mostly devoted to processing and absorption of small molecules. Our study also shows that many digestive genes are organized in genomic clusters in which each gene tends to display a distinct expression pattern. This mode of gene organization could provide a mechanism to optimize gene expression in various gut regions. Our study also confirms that the immune system of the gut is compartmentalized with a clear dichotomy between endodermal and ectodermal portions of the gastrointestinal tract. Although the global organization of mammalian and insect guts is not conserved, similar functional sequences can be observed as shown by the position of the region dedicated to iron absorption (R4a) downstream of the acidic compartment (R3) as observed in mammals. Although digestion is central to an organism's health, it remains poorly characterized at the genetic level. Our present study is a starting point to dissect the molecular mechanisms underlying the digestive process in *Drosophila*. An ultimate goal would be to understand the logic of midgut compartmentalization and how epithelium architecture, enzyme production, and digestive properties are coordinated to achieve optimal digestion.

Establishment and Stability of Gut Regionalization

Most enhancer traps that produce patterned expression profiles in the adult gut exhibit similar expression properties in the larval midgut, albeit in a different sequence (data not shown). This implies that the overall patterning of the larval and adult midgut is different, possibly reflecting the different lifestyles of larvae and adults. It would be interesting to analyze to what extent gut compartmentalization is conserved among different insect species and whether molecular mechanisms governing the establishment and maintenance of gut regions are conserved.

Our study shows that the compartmentalization of the adult midgut is established within the first 2 days posteclosion and maintained throughout adult life. The intestinal patterning is primarily defined by regional identity cues, and not by environmental factors. In addition, it can be fully restored following a strong disturbance of gut homeostasis. This indicates that the molecular mechanisms underlying regional identity are actively maintained to ensure normal enterocyte differentiation and gut morphology. However, the molecular mechanisms that maintain intestinal regionalization as well as the role of ISCs in this process remain poorly understood. Further studies are required to unravel how regional molecular players govern distinct ISC differentiation programs to generate various enterocyte types along the gut. Recently, Strand and Micchelli have shown that the middle midgut contains a specific population of ISCs called "gastric stem cells" (Strand and Micchelli, 2011), suggesting that differences in local stem cell populations could generate regions with specific identity. Conversely, the surrounding tissues, such as the visceral muscles, may influence stem cell lineage differentiation into specific enterocyte types to maintain intestinal regionalization.

Several studies have shown that aging alters adult midgut properties (Biteau et al., 2008; Choi et al., 2008). Consistent with these observations, our study indicates that the capacity to maintain a proper intestinal regionalization decreases with age. This raises the hypothesis that loss of intestinal patterning could contribute to aging and thus affect lifespan. Our study also shows that disruption of gut compartmentalization affects gut homeostasis leading to an increase in stem cell proliferation and a higher immune response. This underlies the role of gut compartmentalization in health and indicates that multiple genetic factors can indirectly disrupt immune tolerance in the gut, a situation that could also prevail in the human gut.

Maintenance of the Adult Gut Regionalization Requires "Developmental" TFs

Several Hox proteins are important for the patterning of the intestine in the *Drosophila* embryo as well as in mammals (Bienz, 1994; Zákány and Duboule, 1999; Kawazoe et al., 2002). In

Drosophila, Labial is the only Hox protein that is expressed in the midgut epithelium during the embryonic development where it is required for the differentiation of copper cells and their maintenance in larvae (Hoppler and Bienz, 1994; Dubreuil et al., 2001). Here, we show that *labial* is also required for the morphological differentiation of copper cells and for the expression of digestive genes in R3 at the adult stage. Although we currently do not know whether these genes are direct targets of Labial, our study suggests that Labial coordinates both copper cell morphology and function. We also identified several other regulators required for R3 gene expression including the pan-midgut TF *GATAe* and another R3-specific TF, the bicoid-related homeobox *Ptx1*. These results suggest that R3 identity is defined by an interplay between pan-midgut and regionalized TFs, a regulatory mechanism that is likely operational in other gut regions. *Labial* and *GATAe* have both been previously identified for their role in gut embryonic development (Dubreuil, 2004; Okumura et al., 2005), whereas here, we show that they are also required for the maintenance of gut regionalization throughout adult life. One possible mechanism to explain how those TFs propagate gut and region identities during adult life could be that once activated, Labial and GATAe sustain their own expression by an autoregulatory loop as previously proposed for the GATA factors elt-7/elt-2, which coordinate the *C. elegans* intestinal gene program (Sommermann et al., 2010). In *C. elegans*, TFs required for early aspects of intestinal development were also shown to activate late-acting genes involved in digestion (Gaudet and Mango, 2002; Sommermann et al., 2010). From an evolutionary point of view, it may be possible that the ancestral function of the TFs that control both the development and function of the gut was to mediate specific digestive functions and that they were only later co-opted in other developmental processes.

The Wnt Pathway Regulates Gene Expression in the Vicinity of Boundaries

Many genes are expressed in a graded manner in the midgut, which may improve gut metabolic activity through the gradual expression of digestive enzymes or transporters (Karasov et al., 2011). Our study points to a potential role for the Wnt pathway in organizing this graded gene expression along the midgut. This is supported by the observations that (i) the gene expression gradients identified with Gal4 enhancer trap lines overlap that of the Wnt pathway reporter *Fz3-RFP*, and (ii) the graded expression of the enhancer trap *113276-Gal4* in R5 is abolished when *pangolin* activity is blocked in enterocytes and is expanded when Wingless is overexpressed. Previous studies have reported that Wingless is produced by visceral muscles and progenitor cells at low levels all along the gut, where it activates Wnt pathway in ISCs (Lin and Xi, 2008; Cordero et al., 2012). In addition, it is produced at high levels in the cardia and in the hindgut proliferation zone nearby the midgut/hindgut junction (Takashima et al., 2008; Singh et al., 2011). This suggests that these boundaries are sources of Wnt ligands and could act as tissue-organizing centers through the induction of Wnt pathway in nearby enterocytes. Future studies should address whether $B_{R2–R3}$ and $B_{R3–R4}$ are also sources of Wnt ligands, as suggested by the graded expression of the *Fz3-RFP* at the vicinity of these boundaries. Studies on intestinal boundaries in mammals indicate that they play a dual role acting both as sphincters and organizing centers as exemplified by the pylorus that generates a gradient of Wnt pathway activity (Li et al., 2009). Futures studies should decipher whether intestinal boundaries in *Drosophila* also play dual roles acting both as sphincters and intestinal-organizing centers.

The homeobox gene *caudal* is also expressed in a graded manner in R4 and R5 showing a broader expression range compared to the *Fz3-RFP* reporter (Figure S6B). The expression of *caudal* was not affected when *pangolin* was silenced in enterocytes (data not shown). This suggests that the Wnt pathway and Caudal act independently to pattern posterior midgut genes. However, an alternative and perhaps more intuitive function of Caudal could be to define the posterior midgut-hindgut territories by setting up the Wnt gradient activity. This would be consistent with the function of *Caudal* during embryonic development where it functions to establish a Wingless-secreting boundary through which normal hindgut formation is mediated (Wu and Lengyel, 1998). This previous study and our data suggest a model that involves two major regulatory steps to subdivide the adult midgut. First, this tissue is compartmentalized into regions separated by major boundaries through the activity of master TFs such as homeobox genes. Second, these main regions are further divided into subregions through the graded activity of secreted morphogens released from these boundaries. In the case of R5, a gradient of Wnt activity established from the midgut/hindgut boundary could subdivide the *Caudal* expression domain in R4c (caudal on, no Wnt activity), R5a (caudal on, low Wnt activity), and R5b (caudal on, high Wnt activity). Such a model could explain the overall organization of the midgut where the position of subregions often correlates with Wnt gradients. It is interesting to note that the overall organization of the midgut appears symmetric around R3 (see Figure 7F). This is well supported by the clustering of our microarray data, which revealed functional similarities between R2 and R4. This symmetry could originate during early gut development when the midgut is formed through the convergent migration of progenitors from foregut and hindgut (Tepass and Hartenstein, 1994).

Concluding Remarks

This study and the associated database (http://flygut.epfl.ch) improve our understanding of insect physiology by providing a detailed atlas that describes the *Drosophila* adult midgut compartments. Additionally, we provide a glimpse into the regulatory mechanisms underlying *Drosophila* midgut regionalization. It indicates that adult intestinal regionalization is achieved through the interplay between pan-midgut and regionalized TFs in concert with the spatial activity of morphogens. Our study has fundamental but also applied significance because the insect gut is a target for pest control and an obligate passage for many insect-borne human diseases. Furthermore, the ancient origin of the gut in metazoan evolution together with similarities in intestinal structures and function between flies and mammals suggest that studies in *Drosophila* could significantly impact the knowledge of regulatory programs underlying gut structure and function in mammals.

EXPERIMENTAL PROCEDURES

Fly Stocks

To perform the gene expression pattern analysis, the F1 progeny derived from crosses between *UAS-nlsGFP* flies and Gal4 enhancer trap flies was raised at 25°C for at least 3 days and moved to a tube containing a filter paper soaked with sucrose solution for 2 hr (to eliminate food fluorescence). For RNAi studies, adults carrying one copy of the Gal4 driver with *Gal80^{ts}* and one copy of the *UAS-dsRNA* were raised at 18°C for 3 days and then moved to 29°C for at least 5 days. The progeny of *Oregon^{R}* flies crossed with *Myo1A-Gal4*, *Gal80^{ts}* was used as wild-type controls. For a description of the fly lines used in this study, see the Extended Experimental Procedures.

Morphometric and Gene Expression Pattern Analyses

The radius of six guts was measured using the Zeiss measurement module and plotted along the entire gut axis. The starting and endpoints of segments expressing GFP were localized and their coordinates reported as a percentage of gut length. In addition, the GFP intensity of each gut was determined quantitatively by analyzing the signal intensity (GFP) along the gut with the Fiji software.

ACCESSION NUMBERS

Raw data and processed files of the microarray analysis can be found at http://flygut.epfl.ch/expressions and at ArrayExpress with accession number E-MTAB-1620.

SUPPLEMENTAL INFORMATION

Supplemental information includes seven figures, Extended Results, and Extended Experimental Procedures and can be found with this article online at http://dx.doi.org/10.1016/j.celrep.2013.04.001.

LICENSING INFORMATION

ACKNOWLEDGMENTS

We acknowledge W.-J. Lee, A. Paululat, C. Nicchitta, L. Pallanck, T. Preat, H. Reichert, A. Debec, J. deNavascues, the National Institute of Genetics, the *Drosophila* Genetic Resource Center, and the *Drosophila* RNAi Screening Center (Harvard) for fly stocks. We thank N.A. Broderick, I. Miguel-Aliaga, J. deNavascues, and A. Martinez Arias for insightful discussions. We thank the BIOP and HCF core Facilities at Ecole Polytechnique Federale Lausanne for help on imaging and histological analyses. This work was supported by FEBS (fellowship to D.O.), the Bettencourt-Scheller Foundation, an ERC Advanced Grant, and the Swiss National Fund (3100A0-12079/1).

Received: November 15, 2012
Revised: March 5, 2013
Accepted: April 2, 2013
Published: May 2, 2013

REFERENCES

Abraham, I., and Doane, W.W. (1978). Genetic regulation of tissue-specific expression of amylase structural genes in *Drosophila melanogaster*. Proc. Natl. Acad. Sci. USA *75*, 4446–4450.

Amcheslavsky, A., Jiang, J., and Ip, Y.T. (2009). Tissue damage-induced intestinal stem cell division in *Drosophila*. Cell Stem Cell *4*, 49–61.

Bienz, M. (1994). Homeotic genes and positional signalling in the *Drosophila* viscera. Trends Genet. *10*, 22–26.

Biteau, B., Hochmuth, C.E., and Jasper, H. (2008). JNK activity in somatic stem cells causes loss of tissue homeostasis in the aging *Drosophila* gut. Cell Stem Cell *3*, 442–455.

Buchon, N., Broderick, N.A., Chakrabarti, S., and Lemaitre, B. (2009a). Invasive and indigenous microbiota impact intestinal stem cell activity through multiple pathways in *Drosophila*. Genes Dev. *23*, 2333–2344.

Buchon, N., Broderick, N.A., Poidevin, M., Pradervand, S., and Lemaitre, B. (2009b). *Drosophila* intestinal response to bacterial infection: activation of host defense and stem cell proliferation. Cell Host Microbe *5*, 200–211.

Chintapalli, V.R., Wang, J., and Dow, J.A.T. (2007). Using FlyAtlas to identify better *Drosophila melanogaster* models of human disease. Nat. Genet. *39*, 715–720.

Choi, N.H., Kim, J.G., Yang, D.J., Kim, Y.S., and Yoo, M.A. (2008). Age-related changes in *Drosophila* midgut are associated with PVF2, a PDGF/VEGF-like growth factor. Aging Cell *7*, 318–334.

Cognigni, P., Bailey, A.P., and Miguel-Aliaga, I. (2011). Enteric neurons and systemic signals couple nutritional and reproductive status with intestinal homeostasis. Cell Metab. *13*, 92–104.

Cordero, J.B., Stefanatos, R.K., Scopelliti, A., Vidal, M., and Sansom, O.J. (2012). Inducible progenitor-derived Wingless regulates adult midgut regeneration in *Drosophila*. EMBO J. *31*, 3901–3917.

Demerec, M. (1950). Biology of *Drosophila* (New York: John Wiley & Sons).

Dimitriadis, V.K. (1991). Fine structure of the midgut of adult *Drosophila auraria* and its relationship to the sites of acidophilic secretion. J. Insect Physiol. *37*, 167–171.

Dubreuil, R.R. (2004). Copper cells and stomach acid secretion in the *Drosophila* midgut. Int. J. Biochem. Cell Biol. *36*, 745–752.

Dubreuil, R.R., Frankel, J., Wang, P., Howrylak, J., Kappil, M., and Grushko, T.A. (1998). Mutations of alpha spectrin and labial block cuprophilic cell differentiation and acid secretion in the middle midgut of *Drosophila* larvae. Dev. Biol. *194*, 1–11.

Dubreuil, R.R., Grushko, T., and Baumann, O. (2001). Differential effects of a labial mutation on the development, structure, and function of stomach acid-secreting cells in *Drosophila melanogaster* larvae and adults. Cell Tissue Res. *306*, 167–178.

Gaudet, J., and Mango, S.E. (2002). Regulation of organogenesis by the *Caenorhabditis elegans* FoxA protein PHA-4. Science *295*, 821–825.

Hakim, R.S., Baldwin, K., and Smagghe, G. (2010). Regulation of midgut growth, development, and metamorphosis. Annu. Rev. Entomol. *55*, 593–608.

Han, Z., Yi, P., Li, X., and Olson, E.N. (2006). Hand, an evolutionarily conserved bHLH transcription factor required for *Drosophila* cardiogenesis and hematopoiesis. Development *133*, 1175–1182.

Hoppler, S., and Bienz, M. (1994). Specification of a single cell type by a *Drosophila* homeotic gene. Cell *76*, 689–702.

Jiang, H., Patel, P.H., Kohlmaier, A., Grenley, M.O., McEwen, D.G., and Edgar, B.A. (2009). Cytokine/Jak/Stat signaling mediates regeneration and homeostasis in the *Drosophila* midgut. Cell *137*, 1343–1355.

Karasov, W.H., Martínez del Rio, C., and Caviedes-Vidal, E. (2011). Ecological physiology of diet and digestive systems. Annu. Rev. Physiol. *73*, 69–93.

Kawazoe, Y., Sekimoto, T., Araki, M., Takagi, K., Araki, K., and Yamamura, K.-I. (2002). Region-specific gastrointestinal Hox code during murine embryonal gut development. Dev. Growth Differ. *44*, 77–84.

Li, X., Udager, A.M., Hu, C., Qiao, X.T., Richards, N., and Gumucio, D.L. (2009). Dynamic patterning at the pylorus: formation of an epithelial intestine-stomach boundary in late fetal life. Dev. Dyn. *238*, 3205–3217.

Lin, G., and Xi, R. (2008). Intestinal stem cell, muscular niche and Wingless signaling. Fly (Austin) *2*, 310–312.

Lin, G., Xu, N., and Xi, R. (2008). Paracrine Wingless signalling controls self-renewal of *Drosophila* intestinal stem cells. Nature *455*, 1119–1123.

Micchelli, C.A., and Perrimon, N. (2006). Evidence that stem cells reside in the adult *Drosophila* midgut epithelium. Nature *439*, 475–479.

Murakami, R., Shigenaga, A., Kiwano, E., Matsumoto, A., Yamaoka, I., and Tanimura, T. (1994). Novel tissue units of regional differentiation in the gut epithelium of *Drosophila*, as revealed by P-element-mediated detection of enhancer. Rouxs Arch. Dev. Biol. *203*, 243–249.

Ohlstein, B., and Spradling, A. (2007). Multipotent *Drosophila* intestinal stem cells specify daughter cell fates by differential notch signaling. Science *315*, 988–992.

Okumura, T., Matsumoto, A., Tanimura, T., and Murakami, R. (2005). An endoderm-specific GATA factor gene, dGATAe, is required for the terminal differentiation of the *Drosophila* endoderm. Dev. Biol. *278*, 576–586.

Olson, E.R., Pancratov, R., Chatterjee, S.S., Changkakoty, B., Pervaiz, Z., and DasGupta, R. (2011). Yan, an ETS-domain transcription factor, negatively modulates the Wingless pathway in the *Drosophila* eye. EMBO Rep. *12*, 1047–1054.

Pédron, T., and Sansonetti, P.J. (2008). Commensals, bacterial pathogens and intestinal inflammation: an intriguing ménage à trois. Cell Host Microbe *3*, 344–347.

Popichenko, D., Sellin, J., Bartkuhn, M., and Paululat, A. (2007). Hand is a direct target of the forkhead transcription factor Biniou during *Drosophila* visceral mesoderm differentiation. BMC Dev. Biol. *7*, 49.

Radtke, F., and Clevers, H. (2005). Self-renewal and cancer of the gut: two sides of a coin. Science *307*, 1904–1909.

Ryu, J.H., Kim, S.H., Lee, H.Y., Bai, J.Y., Nam, Y.D., Bae, J.W., Lee, D.G., Shin, S.C., Ha, E.M., and Lee, W.J. (2008). Innate immune homeostasis by the homeobox gene caudal and commensal-gut mutualism in *Drosophila*. Science *319*, 777–782.

Schuijers, J., and Clevers, H. (2012). Adult mammalian stem cells: the role of Wnt, Lgr5 and R-spondins. EMBO J. *31*, 2685–2696.

Shanbhag, S., and Tripathi, S. (2009). Epithelial ultrastructure and cellular mechanisms of acid and base transport in the *Drosophila* midgut. J. Exp. Biol. *212*, 1731–1744.

Singh, S.R., Zeng, X., Zheng, Z., and Hou, S.X. (2011). The adult *Drosophila* gastric and stomach organs are maintained by a multipotent stem cell pool at the foregut/midgut junction in the cardia (proventriculus). Cell Cycle *10*, 1109–1120.

Sommermann, E.M., Strohmaier, K.R., Maduro, M.F., and Rothman, J.H. (2010). Endoderm development in *Caenorhabditis elegans*: the synergistic action of ELT-2 and -7 mediates the specification→differentiation transition. Dev. Biol. *347*, 154–166.

Stainier, D.Y. (2005). No organ left behind: tales of gut development and evolution. Science *307*, 1902–1904.

Strand, M., and Micchelli, C.A. (2011). Quiescent gastric stem cells maintain the adult Drosophila stomach. Proceedings of the National Academy of Sciences *108*, 17696–17701.

Takashima, S., Mkrtchyan, M., Younossi-Hartenstein, A., Merriam, J.R., and Hartenstein, V. (2008). The behaviour of *Drosophila* adult hindgut stem cells is controlled by Wnt and Hh signalling. Nature *454*, 651–655.

Tepass, U., and Hartenstein, V. (1994). Epithelium formation in the *Drosophila* midgut depends on the interaction of endoderm and mesoderm. Development *120*, 579–590.

Terra, W.R. (1990). Evolution of digestive systems of insects. Annu. Rev. Entomol. *35*, 181–200.

Terra, W.R., and Ferreira, C. (1994). Insect digestive enzymes: properties, compartmentalization and function. Comp. Biochem. Physiol. *109*, 1–62.

Wang, X., Wu, Y., and Zhou, B. (2009). Dietary zinc absorption is mediated by ZnT1 in *Drosophila melanogaster*. FASEB J. *23*, 2650–2661.

Wu, L.H., and Lengyel, J.A. (1998). Role of caudal in hindgut specification and gastrulation suggests homology between *Drosophila* amnioproctodeal invagination and vertebrate blastopore. Development *125*, 2433–2442.

Yonge, C.M. (1937). Evolution and adaptation in the digestive system of the Metazoa. Biol. Rev. Camb. Philos. Soc. *12*, 87–114.

Zákány, J., and Duboule, D. (1999). Hox genes and the making of sphincters. Nature *401*, 761–762.